www.czasopisma.pan.pl PAN www.journals.pan.pl
Opto-Electronics Review 25 (2017) 269–273

Contents lists available at ScienceDirect

Opto-Electronics Review

journal homepage: http://www.journals.elsevier.com/opto-electronics review

Highly-efficient fully-fiberized mid-infrared differential frequency generation source and its application to laser spectroscopy

K. Krzempek*, G. Dudzik, A. Hudzikowski, A. Gluszek, K. Abramski

Faculty of Electronics, Laser & Fiber Electronics Group, Wroclaw University of Science and Technology, Wybrzeze Wyspianskiego 27, 50-370, Wroclaw, Poland

ARTICLE INFO

Article history:
Received 14 June 2017
Received in revised form 1 August 2017
Accepted 8 August 2017
Available online 11 September 2017

Keywords:
Fiber laser
Laser spectroscopy
Wavelength modulation spectroscopy
Nonlinear frequency mixing

ABSTRACT

Widely-tunable, fully-monolithic, mid-infrared (mid-IR) deference frequency generation source (DFG) is presented. By using a custom designed fiber-pigtailed periodically poled lithium niobate (PPLN) crystal module the *idler* beam was generated with an efficiency of 21%/W, yielding 2.6 mW of optical output power. The proposed all-fiber configuration radically simplified the optical frequency conversion setup, making it robust and easily configurable. The usefulness of the constructed source was verified by performing simultaneous wavelength modulation spectroscopy (WMS) laser trace gas detection of methane, near 2999 cm^{-1}, and ethane, near 2997 cm^{-1}, via two independently generated, tunable *idler* beams.

Introduction

Laser sources operating in the mid-infrared (mid-IR) wavelength region have been in the spotlight for the last decade, receiving a lot of attention from the laser community. This lead to their rapid development and simultaneously a great amount of research papers being published, focusing on physical principles of operation, production process improvement and applications. The ongoing thrive of mid-IR laser sources is mainly driven by the fact that the wavelength region of their operation is rich in strong fundamental vibration and associated rotational-vibrational absorption bands of many molecules [1]. This fact connected with the recent rapid technological progress in robust, low-power laser sources capable of targeting those absorption bands triggered the development of selective and sensitive laser spectroscopy-based sensors [2–6]. A relatively narrow spectral region, spanning between 3 and 3.5 μm is particularly interesting, because it holds strong fingerprints of hydrocarbons – e.g. methane, ethane acetylene and others [7–9]. Implementing laser-based detection techniques in that particular wavelength region requires a coherent source that can be swept across the target analyte. Experimental realizations of such sensors include using intraband cascade lasers (ICL) diodes [10–12], frequency conversion-based sources [13–15] or recently developed fiber-based sources [16]. Each approach has their pros and cons. The ICL's are compact and relatively easy to combine in laser spectroscopy setups, but at the same time provide a limited tuning range. Therefore, simultaneous detection of more than one target analyte usually requires using independent laser sources, each specifically tailored to a chosen molecule transition [17]. This complicates the sensor layout and multiplies the cost of deployment. The frequency conversion-based laser sources are a well-developed branch of mid-IR coherent sources. Despite known for their complexity, have been widely used in spectroscopy applications. Mainly due to their flexibility, very wide tuning range and the possibility of using fiber-based lasers as *pump* and *signal* sources, proving to be an alternative for semiconductor-based lasers [18]. DFG-based mid-IR sources capable of generating radiation in the 3.4 μm wavelength region are particularly interesting, due to the fact, that the nonlinear frequency generation process can be easily achieved by mixing 1 μm and 1.5 μm waves in widely available periodically poled lithium niobate (PPLN) crystals. The beams required in the nonlinear process can be delivered by non-complex and efficient fiber-based sources, using erbium (Er) and ytterbium (Yb) doped active fibers. The down-side of standard, bulk crystal-based DFG sources is the poor efficiency. Achieving several miliwats of *idler* beam requires Watt-level *signal* and *pump* beams being delivered to the crystal structure [14]. Moreover, complex optical setups are required for appropriate input beam shaping and coupling into the crystal, thus air-tight housing is a necessity to prevent contamination in an out-of-lab operation.

In his paper we report on a DFG-based mid-IR laser which is free of the most common drawbacks listed above. The proposed source is fully-monolithic, widely-tunable, highly-efficient, requires minimal number of optical components and is using emission of simple and inexpensive all-fiber lasers in the frequency mixing process. By incorporating a custom-designed fiber-coupled PPLN module the

* Corresponding author.
E-mail address: karol.krzempek@pwr.edu.pl (K. Krzempek).

http://dx.doi.org/10.1016/j.opelre.2017.08.002
1230-3402/

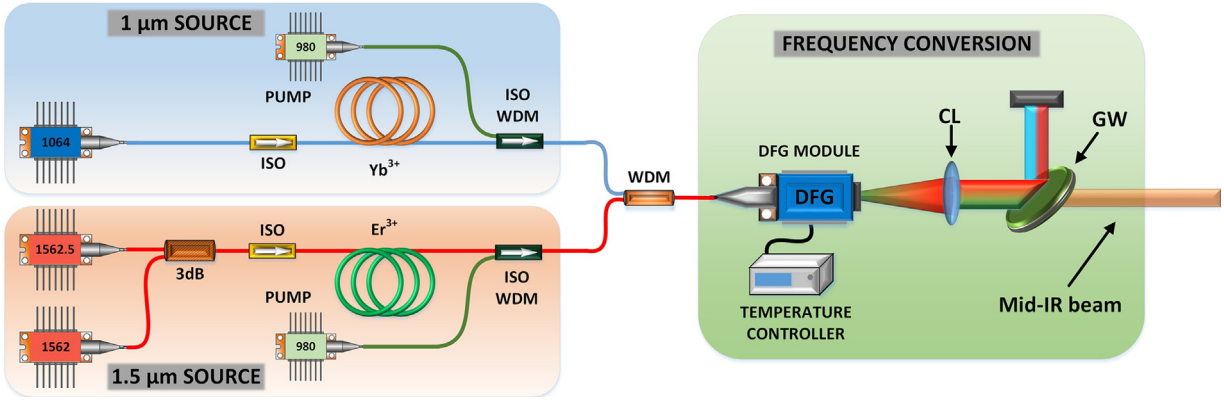

Fig. 1. Experimental setup of the fully monolithic, widely tunable all-fiber mid-IR source. 1562, 1562.5, 1064–DFB seed laser diodes (with wavelength as stated on the component), 980–980 nm, 600 mW singlemode pump diode, ISO – fiber isolator, ISO WDM – hybrid fiber component, Er^{3+} – 20 cm long active fiber doped with erbium ions, Yb^{3+} – 20 cm long active fiber doped with ytterbium ions, WDM – wavelength division multiplexer, DFG – difference frequency generation module, CL – collimating lens, GW – germanium window. All fiber components and fibers were polarization maintaining.

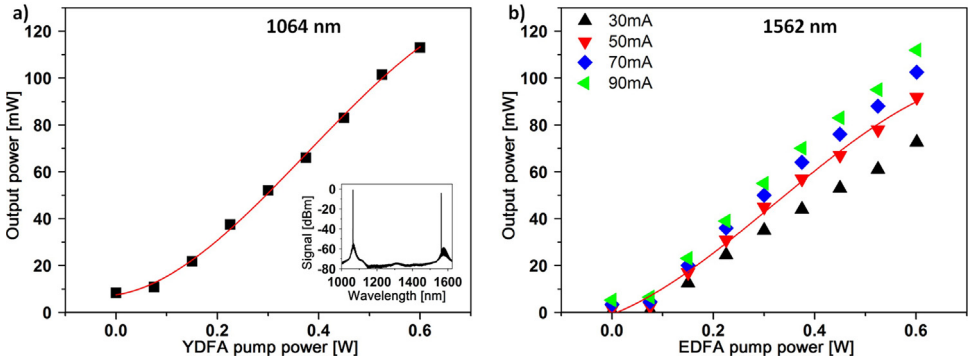

Fig. 2. Output power of both fiber amplifiers used in the experiment plotted in function of pump power delivered to the active fiber. Plot a) shows the performance of the YDFA with an inset presenting the optical spectrum registered after the WDM coupler, at maximum pump power delivered to both amplifiers. Plot b) shows output power of EDFA for 4 different 1562 seed input powers (currents set at the laser driver).

number of optical components required in the setup was reduced to a single lens collimating the *idler* output beam and a germanium filter. The proposed design reach a conversion efficiency of 21%/W, due to the waveguided (WG) structure of the PPLN crystal enclosed in the fiber-coupled frequency conversion module, at the same time reducing long-term power instabilities.

The usefulness of the constructed all-fiber mid-IR source was tested by setting-up a wavelength modulation spectroscopy-based (WMS) sensor capable of simultaneously targeting methane (CH_4) and ethane (C_2H_6) transitions, located at 2999 and 2997 cm^{-1}, respectively.

Mid-infrared source architecture

Experimental setup of the widely-tunable, fully-fiberized mid-IR source is depicted in Fig. 1. It can be divided into two main sections – low power near-IR seed sources and fiber amplifiers and the frequency conversion section. The DFG process in PPLN crystals requires the input beams to be linearly polarized. The nonlinear conversion efficiency strongly depends on the precision of polarization vector orientation in respect to the crystal axis. Any drift of this orientation or deviation from linear polarization will result in output power drop. Because the proposed mid-IR source will be tested in a laser spectroscopy configuration, any fluctuation of the output power would be considered as a noise source. Thus, the entire source has been constructed using widely available polarization maintaining (PM) fibers and components, which minimize polarization instability issues.

The optical beams used in the frequency conversion were delivered from standard, distributed feedback (DFB) seed laser diodes. We have used three diodes lasing at 1064 nm (referred as *pump* beam in the frequency conversion process), 1562 nm and 1562.5 nm (referred as *signal* beams), respectively. Separate seed diodes at the 1.5 um wavelength region were used to generate independently tunable and modulated *idler* mid-IR beams, which will later be used to simultaneously target strong absorption lines of ethane and methane. The emission of those lasers was combined via a PM 3 dB fiber coupler and coupled into an Er-doped fiber amplifier (EDFA) to boost the output power. Similarly, the 1064 nm diode was amplified in an Yb-doped fiber amplifier (YDFA). Both amplifiers were built in a standard linear amplifier configuration. The seed light was coupled through an isolator to a wavelength division multiplexer (WDM) which also coupled a 600 mW, 980 nm singlemode pump laser diode to the active fiber (both active fibers were 20 cm long). The WDM couplers were of a filter-type. The pump beams were reflected back to the active fibers, forming backward-pumped configurations, for both amplifiers. Each amplifier was terminated with a second isolator, preventing any back-scattered light distorting their operation. The seed diodes and the pump diodes were controlled by an all-in-one current and temperature controllers (Thorlabs CLD 1015). Outputs of EDFA and YDFA were combined in a single fiber via a PM-WDM coupler designed for 1 um and 1.5 um light. The performance of both amplifiers is shown in Fig. 2, where output power was plotted in function of pump power delivered to the amplifier (measured with Thorlabs S401C power meter after the WDM coupler). Insets show optical spectrum registered at

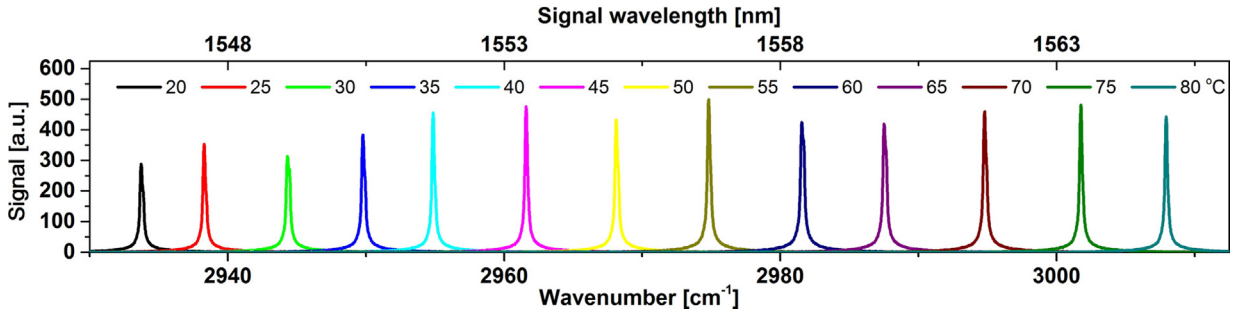

Fig. 3. Mid-IR idler beam tuning range plotted in function of the crystal temperature and input signal wavelength. Temperature of the crystal was tuned accordingly to the wavelength of the signal laser. A widely tunable laser source was used as the signal source. The mid-IR emission was measured with an FTIR spectrometer.

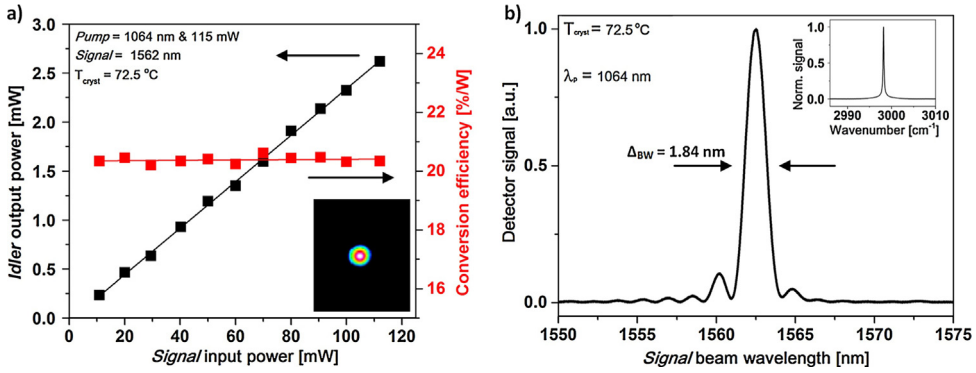

Fig. 4. Idler output power plotted in function of signal power delivered to the frequency conversion module (the pump input power was kept at 115 mW) – figure a). Inset shows idler beam profile registered at maximum input powers. Figure b) shows the measured nonlinear conversion bandwidth. Inset shows optical spectrum of generated idler beam registered for maximum pump and signal input powers.

the output with both amplifiers running at maximum pump power (registered with ANDO, AQ6317B).

During the measurement the 1064 nm seed diode was delivering 10 mW, while the ~1562 nm diodes delivered a total of 9 mW (measured after the 3 dB coupler). Under maximum pump power (600 mW) the amplifiers were capable of delivering 115 and 112 mW, at 1064 nm and 1562 nm, respectively. The amplified beams, combined in a single fiber, were delivered to the frequency conversion section of the reported mid-IR source. The nonlinear process of mixing amplified near-IR optical beams was achieved in a custom-designed, fiber-pigtailed DFG module (NTT Photonics). The module consists of a 40-mm-long periodically poled lithium niobate (PPLN) crystal with a single waveguide (WG) channel etched onto its structure. The crystal is mounted on a Peltier module, which enables thermal stabilization of the nonlinear medium at a desired temperature, fulfilling the quasi-phase-matching conditions [19]. The beam exiting the DFG module was collimated using a single plano-convex lens (f = 20 mm, calcium-fluoride, anti-reflection coated for mid-IR wavelengths) and separated from the unabsorbed pump and signal beams by a 5 mm thick un-coated germanium window. The parameters were designed and the module was produced according to our specification to possess several crucial parameters. The period of the WG channel ($\Delta = \sim 30.3\ \mu m$) was chosen to fully utilize the broadband amplification region of standard EDFA's. By simply tuning the temperature of the crystal (in the safe temperature range of 20–80 °C) efficient quasi-phase-matching of a *signal* wavelength ranging from 1540 to 1565 nm, with a *pump* wavelength set to 1064 nm, is feasible. The experimentally verified tuning characteristics of the generated *idler* mid-IR beam is depicted in Fig. 3.

In the measurement we have used a widely tunable laser source (ANDO AQ4321A) as the *signal* beam and the *pump* beam was the 1064 nm seed laser. The mid-IR emission was measured using a FTIR spectrometer (Nicolet IS50). Worth noting is the fact, that the constructed all-fiber mid-IR source, which was built on basis of inexpensive and widely available fiber components, was capable of generating mid-IR radiation tunable in the range of 2930–3010 cm^{-1}. The slight differences in amplitude of each registered emission originate mainly from the gain characteristics of the EFDA used to boost the emission of the tunable laser source.

The WG structure etched onto the 40-mm-long PPLN crystal ensures that both beams taking part in the nonlinear mixing process (*pump* and *signal*) are tightly and collinearly guided throughout the crystals total length. This optimizes their overlap and minimizes the walk-off-related conversion efficiency drops. In Fig. 4a) the *idler* output power was plotted in function of *signal* power delivered to the DFG module (*pump* power was kept at 115 mW). The output power was measured after the germanium filter. The inset shows *idler* beam profile registered at maximum input powers, with a mid-IR beam profiling camera (DataRay, WinCamD). In Fig. 4b) the nonlinear conversion bandwidth (BW) was plotted, along with *idler* optical spectrum registered for maximum input powers of the *pump* and *signal* beams (inset). The BW was measured for constant crystal temperature, input powers and *pump* wavelength.

Under maximum input powers, 115 mW and 112 mW, for *pump* and *signal* input beams, the fully fiberized source was capable of generating 2.6 mW of CW optical power at the *idler* frequency (~2998.5 cm^{-1}). Due to the all-fiber design and the WG-PPLN, the nonlinear frequency conversion efficiency reached nearly 21%/W, which is an increase of nearly three orders of magnitude, compared to similar setups incorporating bulk, non-WG-PPLN crystals for DFG with fiber-based laser sources [14]. According to the manufacturer, the DFG module is capable of withstanding 500 mW of CW optical input power. Therefore, if seeded with *pump* and *signal* beams with 250 mW of power each, the generated *idler* beam would reach more than 13.1 mW. To enable simultaneous, efficient generation of sev-

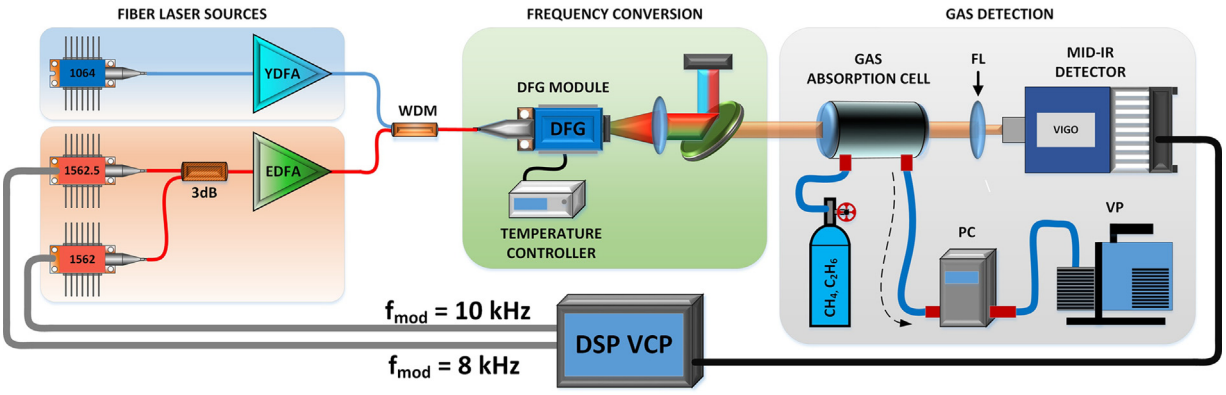

Fig. 5. Wavelength modulation spectroscopy (WMS) methane and ethane detector setup. FL – focusing lens, PC – pressure controller, VP – vacuum pump, DSP VCP – custom developed digital signal processing-based versatile control platform, serving as a signal generator and signal acquisition and analysis tool.

eral, independently tunable *idler* beams via multiple *signal* seeding the crystal is required to have a sufficiently wide frequency conversion bandwidth (conjointly covering all the *signal* beams at a fixed crystal temperature), which is typically inversely proportional to the length of the nonlinear PPLN medium [20]. The experimentally measured full width at half maximum (FWHM) conversion bandwidth was 1.84 nm (for the *signal* wavelength), which is sufficient to simultaneously target several absorption lines of hydrocarbons in the ~3000 cm^{-1}.

Wavelength modulation spectroscopy application

The usability of the fully-monolithic, all-fiber mid-IR laser source was experimentally verified in a standard WMS trace gas detection configuration. The sensor setup is depicted in Fig. 5. The generated, collimated and filtered *idler* beam was transmitted through a 20 cm-long gas absorption tube (mid-IR AR-coated, wedged CaF_2 windows at input and output). The gas cell has been flushed with 200 ppm methane (CH_4) and 50 ppm ethane (C_2H_6) from calibration cylinders. The pressure inside the cell was controlled and stabilized by a controller (MKS, 640B) working in a downstream configuration, terminated by a vacuum pump. The *idler* beam exiting the gas absorption cell was focused onto a thermoelectrically cooled mercury cadmium telluride (MCT) detector (Vigo, PVI4TE), via a 20 mm focal-length CaF_2 lens. The free-space (in air) propagation of the *idler* beam has been intentionally minimized, reaching approximately 20 cm. To ensure the sensitive MCT detector would not be saturated, the EDFA was pumped with just 100 mW, while the YDFA was not pumped, thus the *idler* beam had an optical power of ~170 μW.

During all measurements the PPLN crystal temperature was stabilized at 72.5 °C, ensuring simultaneous, optimal quasi-phase matching and nearly equal output powers for both down-converted 1.5 μm *signal* wavelengths.

During the measurements the temperatures of the 1.5 μm seed lasers were finely tuned to ensure the two generated *idler* frequencies will separately target strong rotational-vibrational transitions of CH_4 and C_2H_6, which are depicted in the Hitran simulation in Fig. 6.

Standard WMS in-lab laser spectroscopy-based gas detectors require a vast number of highly-sophisticated, sensitive and expensive apparatus – laser diode drivers, signal generators, low-noise amplifiers and lock-in amplifiers for phase-sensitive detection. This fact limits the deployment of trace gas measurement devices in real-life, out-of-lab applications. We have addressed this issue by designing and building a custom, all-in-one versatile electronic detection system (VCP). It is based on a Cortex M7 microcontroller, capable of floating point unit operations. The processor

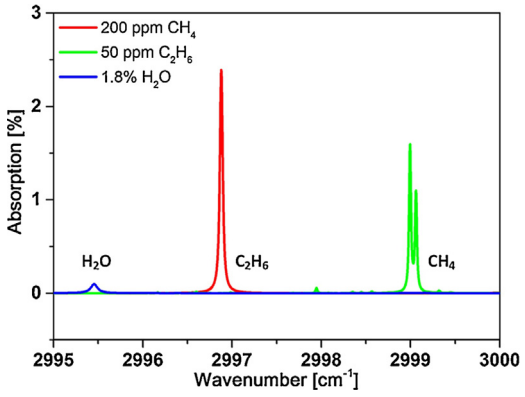

Fig. 6. Hitran simulation of 50 ppm ethane, 200 ppm methane and 1.8% water vapor absorption lines for an interaction length of 20 cm at 100 Torr pressure.

is connected to a custom, low noise compact front end circuit. It has two separate input and output channels. The output ports have programmable gain amplifiers, antialiasing filters and 16-bits-resolution, 1 mega sample analog-to-digital (ADC) and digital-to-analog (DAC) converters. The microcontroller has four implemented lock-in amplifiers, filter banks and two direct digital signal synthesizers. It is fully configurable via 4.3" touch TFT display which also serves as a display for the measurements. The VCP can be connected to a PC via a USB port to gather the measurement data via a LabView interface. More detailed description of the DSP VCP can be found in our previous work [21]. In the reported sensor configuration the VCP was responsible for both the absorption signal aggregation (by analyzing the electric signal for the MCT detector) and for generating signals driving the 1.5 μm seed diodes, thus permitting WMS-based gas detection. The proposed gas detector configuration was designed to highlight the advantages of frequency conversion-based mid-IR sources.

The modular, all-fiber configuration permits multi-*idler* generation, therefore enables simultaneous and independent detection of several gas analytes. Moreover, the wide tuning range covers a wavelength region known for including strong ro-vibrational transitions of many hydrocarbons [22]. Additionally, because the synchronically generated *idler* beams will be intrinsically collinear, multi-species-detection can be easily implemented in a standard WMS detection configuration, what was experimentally verified by us in a proof-of-concept experiment. We propose a configuration which uses a single MCT detector for simultaneous retrieval of methane and ethane 2*f* absorption signals. This technique required dissimilar sine waves modulated onto the current driving the 1.5 μm *signal* seed lasers. The VCP was set to generate 8 kHz

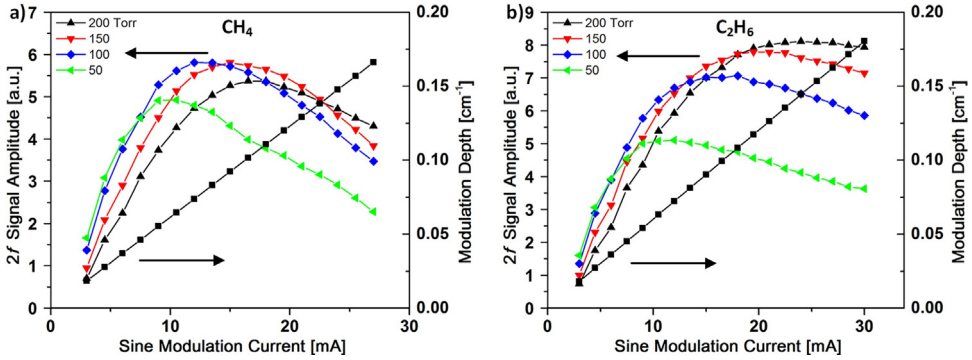

Fig. 7. 2*f* detection signal for 200 ppm methane – a) and 50 ppm ethane – b) plotted in function of sine signal amplitude modulating the signal seed diodes. The measurements were taken for four pressure values.

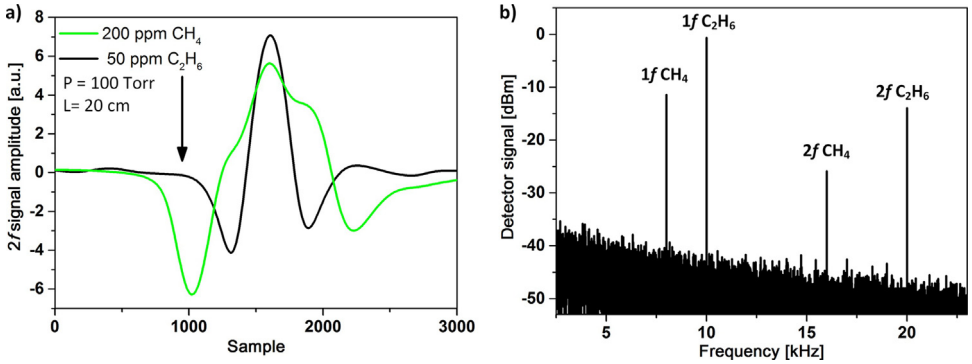

Fig. 8. 2*f* absorption signal registered simultaneously for a 20 cm long cell filled with 200 ppm of methane and 50 ppm of ethane, at 100 Torr pressure, averaged 40 times – a), detector signal analyzed by an RF spectrum analyzer, showing 1*f* and 2*f* absorption signals of both molecules detectable at the same time – b).

and 10 kHz sine signals on two independent outputs, which were coupled to the modulation input of 1.5 μm *signal* diode drivers (depicted in Fig. 5). Optimal WMS detection parameters were determined experimentally by performing a set of measurements depicted in Fig. 7.

Based on the measurements depicted in Fig. 7, optimum parameter values could be determined. The 2*f* signal amplitudes for both molecules had a clear maximum at particular modulation current amplitudes and pressures. Nevertheless, because the sensor was designed to measure methane and ethane in a common gas absorption tube, the optimal pressure had to be a compromise, and was stabilized at 100 Torr during measurements. Both *signal* diodes were set to a base current of 55 mA, approximately at half of their maximum current. The *signal* diode, used to target methane particles (1562.5 nm), via down-converted *idler* beam, was modulated with a 8 kHz sine wave, resulting in a 12 mA peak-peak current modulation. The *signal* diode targeting the ethane particles (1562 nm) was modulated with a 10 kHz sine wave, resulting in a 17 mA peak-peak current modulation. Sweeping through the absorption lines was achieved by adding an additional 5 Hz, 30 mA, triangular shaped current modulation to both *signal* diodes. During the measurements the *pump* diode was set at 100 mA base current with an temperature stabilized near 20.8 °C, generating a 10 mW CW beam at ~1064 nm. Having set all parameters we performed WMS measurements of 200 ppm methane and 50 ppm ethane under 100 Torr, in a 20 cm long absorption tube. The simultaneously registered 2*f* absorption spectra of methane and ethane are depicted in Fig. 8a). Fig. 8b) presents RF signal registered with an spectrum analyzer, showing clear methane WMS signals at 1*f* = 8 kHz, 2*f* = 16 kHz, and ethane signals at 1*f* = 10 kHz, 2*f* = 20 kHz (registered when the *signal* diodes were parked close to the peak of absorption). The VCP was sampling the 2*f* signal at a 100 kHz rate and averaging the gathered signal 40 times. The difference of registered lineshapes [Fig. 8a)] originates from the fact, that the methane transition located at 2999 cm^{-1} consists of 2 individual absorption lines, which clearly separate at a pressure of 100 Torr, while the ethane transition is a single peak (see Fig. 6). The RF signal plotted in Fig. 8b) confirms that the reported mid-IR source was capable of simultaneous detection of two independent absorption lines. By flushing the absorption cell with pure nitrogen (N_2) we measured the noise floor in the vicinity of the targeted absorption profiles. The 1σ signal-to-noise ratio (SNR) was 244 and 285, for methane and ethane, respectively. This equals to a minimum detection limit of 160 ppb × m for CH_4 and 35 ppb × m for C_2H_6. The difference in the obtained limits is connected with the residual amplitude modulation (RAM) present in the baseline [23]. Although the crystal was coated for all wavelengths taking part in the conversion process, the reflections on both ends of the crystal are responsible for a fringe pattern, constantly observable in the 2*f* WMS signal. The observed RAM is the main obstacle for achieving lower detection limits.

The relative position of the sinusoidal-shaped fringe pattern is dependent on the nonlinear crystal temperature, therefore future improvements to the constructed source will involve implementing a measurement routine with simultaneous crystal temperature sweep. Synchronizing the temperature sweep with an appropriate averaging algorithm should cancel-out most of the fringes, and, therefore, enable achieving lower minimum detection limits.

Conclusions

In this letter a first demonstration of using a fully-fiberized, DFG-based mid-IR source in a simultaneous methane and ethane WMS-based gas detection setup was described. By utilizing a custom-designed fiber-pigtailed frequency conversion module a

setup allowing simultaneous down-converting of emission of two ~1.5 μm signal diodes could be built in an all-fiber configuration, significantly simplifying the source architecture. Despite the low complexity, the source was robust and achieved a nonlinear conversion efficiency of nearly 21%/W, yielding over 2.6 mW of CW mid-IR beam near 3.4 μm. The DFG-module was capable of efficient quasi-phase matching *signal* wavelengths stretching over the entire efficient Er-doped fiber amplification curve, thus enabling easy tuning of the generated *idler* beam across a vast 2930–3010 cm^{-1} wavenumber range. The usefulness of the constructed mid-IR source was elaborated in gas detection application using WMS technique and a 20 cm-long gas absorption tube.

The sensor was capable of simultaneous detection of methane and ethane molecules in a single MCT detector setup via down-converting independently modulated *signal* beams. The achieved detection limits reached 160 ppb × m and 35 ppb × m, for methane and ethane, respectively.

Funding

Polish Ministry of Science and Higher Education (MNiSW) (IP2014 021773).

References

[1] R.F. Curl, F.K. Tittel, Tunable infrared laser spectroscopy, annual reports section 'C', Phys. Chem. 98 (2002) 219–272.
[2] A.V. Bernatskiy, V.V. Lagunov, V.N. Ochkin, S.N. Tskhai, Study of water molecule decomposition in plasma by diode laser spectroscopy and optical actinometry methods, Laser Phys. Lett. 13 (2016) 075702.
[3] D. Kumar, S. Gautam, S. Kumar, S. Gupta, H.B. Srivastava, S.N. Thakur, R.C. Sharma, Ultrasensitive photoacoustic sensor based on quantum cascade laser spectroscopy, Spectrochim. Acta Part A Mol. Biomol. Spectrosc. 176 (2017) 47–51.
[4] T. Moguilnaya, I. Suminov, S. Ignatov, Detecting presence of live and dead pathogenic organisms in water and the water solutions by laser spectroscopy, Laser Phys. Lett. 14 (2017) 055601.
[5] J. Westberg, L.A. Sterczewski, G. Wysocki, Mid-infrared multiheterodyne spectroscopy with phase-locked quantum cascade lasers, Appl. Phys. Lett. 110 (2017) 141108.
[6] C. Zheng, W. Ye, N.P. Sanchez, C. Li, L. Dong, Y. Wang, R.J. Griffin, F.K. Tittel, Development and field deployment of a mid-infrared methane sensor without pressure control using interband cascade laser absorption spectroscopy, Sens. Actuators B: Chem. 244 (2017) 365–372.
[7] P. Kluczynski, M. Jahjah, L. Nähle, O. Axner, S. Belahsene, M. Fischer, J. Koeth, Y. Rouillard, J. Westberg, A. Vicet, S. Lundqvist, Detection of acetylene impurities in ethylene and polyethylene manufacturing processes using tunable diode laser spectroscopy in the 3-μm range, Appl. Phys. B 105 (2011) 427.
[8] K. Krzempek, M. Jahjah, R. Lewicki, P. Stefański, S. So, D. Thomazy, F.K. Tittel, CW DFB RT diode laser-based sensor for trace-gas detection of ethane using a novel compact multipass gas absorption cell, Appl. Phys. B 112 (2013) 461–465.
[9] S. Lundqvist, P. Kluczynski, R. Weih, M. von Edlinger, L. Naehle, M. Fischer, A. Bauer, S. Höfling, J. Koeth, Sensing of formaldehyde using a distributed feedback interband cascade laser emitting around 3493 nm, Appl. Opt. 51 (2012) 6009–6013.
[10] K. Krzempek, R. Lewicki, L. Nähle, M. Fischer, J. Koeth, S. Belahsene, Y. Rouillard, L. Worschech, F.K. Tittel, Continuous wave, distributed feedback diode laser based sensor for trace-gas detection of ethane, Appl. Phys. B 106 (2012) 251–255.
[11] C. Li, L. Dong, C. Zheng, F.K. Tittel, Compact TDLAS based optical sensor for ppb-level ethane detection by use of a 3.34 μm room-temperature CW interband cascade laser, Sens. Actuators B: Chem. 232 (2016) 188–194.
[12] L. Liu, B. Xiong, Y. Yan, J. Li, Z. Du, Hollow waveguide-enhanced mid-infrared sensor for real-time exhaled methane detection, IEEE Photonics Technol. Lett. 28 (2016) 1613–1616.
[13] M. Nikodem, K. Krzempek, R. Karwat, G. Dudzik, K. Abramski, G. Wysocki, Chirped laser dispersion spectroscopy with differential frequency generation source, Opt. Lett. 39 (2014) 4420–4423.
[14] K. Krzempek, G. Sobon, K.M. Abramski, DFG-based mid-IR generation using a compact dual-wavelength all-fiber amplifier for laser spectroscopy applications, Opt. Express 21 (2013) 20023–20031.
[15] D. Richter, A. Fried, B.P. Wert, J.G. Walega, F.K. Tittel, Development of a tunable mid-IR difference frequency laser source for highly sensitive airborne trace gas detection, Appl. Phys. B 75 (2002) 281–288.
[16] C.R. Petersen, U. Møller, I. Kubat, B. Zhou, S. Dupont, J. Ramsay, T. Benson, S. Sujecki, N. Abdel-Moneim, Z. Tang, D. Furniss, A. Seddon, O. Bang, Mid-infrared supercontinuum covering the 1. 4–13. 3 μm molecular fingerprint region using ultra-high NA chalcogenide step-index fibre, Nat. Photonics 8 (2014) 830–834.
[17] C. Zheng, W. Ye, N.P. Sanchez, A.K. Gluszek, A.J. Hudzikowski, C. Li, L. Dong, R.J. Griffin, F.K. Tittel, Infrared dual-gas CH4 C2H6 sensor using two continuous-wave interband cascade lasers, IEEE Photonics Technol. Lett. 28 (2016) 2351–2354.
[18] F. Keilmann, S. Amarie, Mid-infrared frequency comb spanning an octave based on an Er fiber laser and difference-frequency generation, J. Infrared Millimeter Terahertz Waves 33 (2012) 479–484.
[19] L.E. Myers, R.C. Eckardt, M.M. Fejer, R.L. Byer, W.R. Bosenberg, J.W. Pierce, Quasi-phase-matched optical parametric oscillators in bulk periodically poled LiNbO3, J. Opt. Soc. Am. B 12 (1995) 2102–2116.
[20] Z. Cao, X. Gao, W. Chen, H. Wang, W. Zhang, Z. Gong, Study of quasi-phase matching wavelength acceptance bandwidth for periodically poled LiNbO3 crystal-based difference-frequency generation, Opt. Lasers Eng. 47 (2009) 589–593.
[21] J. Wojtas, A. Gluszek, A. Hudzikowski, K.F. Tittel, Mid-infrared trace gas sensor technology based on intracavity quartz-enhanced photoacoustic spectroscopy, Sensors 17 (2017) 513.
[22] A.E. Klingbeil, J.B. Jeffries, R.K. Hanson, Temperature-dependent mid-IR absorption spectra of gaseous hydrocarbons, J. Quant. Spectrosc. Radiat. Transfer 107 (2007) 407–420.
[23] A.L. Chakraborty, K. Ruxton, W. Johnstone, M. Lengden, K. Duffin, Elimination of residual amplitude modulation in tunable diode laser wavelength modulation spectroscopy using an optical fiber delay line, Opt. Express 17 (2009) 9602–9607.